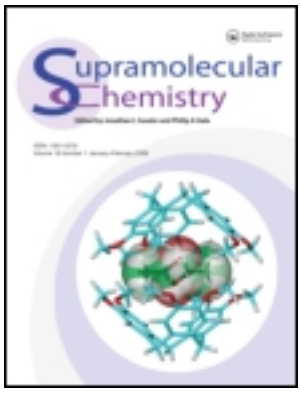

Supramolecular Chemistry
Publication details, including instructions for authors and subscription information:
http://www.tandfonline.com/loi/gsch20

# Supramolecular self-assembled nanowires by the aggregation of a protoporphyrin derivative in low-polarity solvents

Sheshanath V. Bhosale [a], Mohan B. Kalyankar [b], Santosh V. Nalage [b], Sidhanath V. Bhosale [b], Cecilia H. Lalander [a] & Steven J. Langford [a]

[a] School of Chemistry, Monash University, Clayton, Vic., 3800, Australia

[b] Department of Organic Chemistry, North Maharashtra University, Jalgaon, Maharashtra, 425001, India

Available online: 01 Jun 2011

To cite this article: Sheshanath V. Bhosale, Mohan B. Kalyankar, Santosh V. Nalage, Sidhanath V. Bhosale, Cecilia H. Lalander & Steven J. Langford (2011): Supramolecular self-assembled nanowires by the aggregation of a protoporphyrin derivative in low-polarity solvents, Supramolecular Chemistry, 23:8, 563-569

To link to this article: http://dx.doi.org/10.1080/10610278.2011.575467

*Supramolecular Chemistry*
Vol. 23, No. 8, August 2011, 563–569

Taylor & Francis
Taylor & Francis Group

# Supramolecular self-assembled nanowires by the aggregation of a protoporphyrin derivative in low-polarity solvents

Sheshanath V. Bhosale[a]*, Mohan B. Kalyankar[b], Santosh V. Nalage[b], Sidhanath V. Bhosale[b], Cecilia H. Lalander[a] and Steven J. Langford[a]

[a]*School of Chemistry, Monash University, Clayton, Vic. 3800, Australia;* [b]*Department of Organic Chemistry, North Maharashtra University, Jalgaon, Maharashtra 425001, India*

(*Received 12 January 2011; final version received 6 March 2011*)

The self-assembly of a simple tetraalkyl-substituted protoporphyrin derivative into fibril wire-like nanostructures from $CHCl_3$/cyclohexane solvent mixes is explored. The protoporphyrin IX derivative is synthesised in two efficient steps by amidation of the two propylenic acid groups followed by a cross metathesis of the vinyl groups using Grubbs' second-generation catalyst. The self-assembly of the functionalised protoporphyrin is sensitive to solvent and under favourable conditions forms 'nanowires' of micrometre length. The nanowires were characterised by absorption and fluorescence spectroscopy, transmission electron microscopy and atomic force microscopy.

**Keywords:** protoporphyrin IX; supramolecular chemistry; nanowires; AFM; TEM



## Introduction

Self-assembly plays an important role in the construction of 1-, 2- and 3-dimensional (1D, 2D and 3D, respectively) architectures on a nanometre-to-millimetre scale through weak but cooperative interactions (*1*). Multiporphyrin arrays having well-defined shapes and dimensions through self-assembly processes provide significant roles in biology, photonics, catalysis, solar energy conversion and energy storage (*2–7*). Various factors are known to influence the aggregate formation of porphyrin molecules in solution, for example peripheral substitution on the porphyrin, the pH of the medium, the presence of surfactants and/or the ionic strength of the medium (*8–17*). The chemical versatility offered by porphyrins (peripheral substitution and metallation) allows the possibility to instruct the self-assembly into ordered geometrical structures such as molecular squares, rods, rings, wires, nanofibres, polymers, ladders, nanospheres and vesicles (*18–24*). Among various aggregates that are reported to involve porphyrin derivatives, two types are found to be important: the H aggregates, i.e. face-to-face arrangement and the J aggregates, i.e. side-by-side arrangement (*26,27*).

Protoporphyrin IX is the iron-free form of hemin and one of the most common of the naturally occurring porphyrins. These natural porphyrins are amphiphilic bearing hydrophobic groups (methyl/vinyl groups) and hydrophilic groups (carboxylic acid groups) antipodally arranged on the periphery. As a result, this compound should, under the right conditions, exhibit amphiphilic phenomena, forming vesicles and bilayers. However, the self-assembled nanostructures of naturally occurring protoporphyrin derivatives have not yet been extensively studied though some organised structures have been fabricated, for example vesicles (*28*), vesicular tubules (*29,30*), micellar fibres (*31*) and a few other controlled structures (*32–34*). Despite these advances, the 1D self-assembly of protoporphyrin molecules into 'nanowires' remains a challenge. It is obvious that under the correct conditions it should be possible to exploit the ability of protoporphyrins to undergo face-to-face stacking using $\pi$ interactions between the aromatic macrocyclic cores in a 1D sense (*20–27*). Cooperative effects from hydrogen bonding or hydrophobic interactions may help facilitate this process. Herein, we report on the fabrication of micrometre-long nanowires using protoporphyrin **1** (Figure 1). Protoporphyrin **1** bears two important features consistent with other methodologies for studying self-assembly – long ( $>$ C10) alkyl chains radiating from a central point and access to a near planar aromatic core.

## Result and discussion

Compound **1** was prepared in two steps from the readily available protoporphyrin IX. In the first step, protoporphyrin **2** is coupled with 1-dodecylamine using (3-(dimethylamino)propyl)ethylcarbodiimide hydrochloride (EDCI) and 1-hydroxybenzo-triazole (HOBt) in dry dimethyl formamide (DMF) at room temperature yielding the bisamide **3** in 88% yield. Cross metathesis of **3** with

*Corresponding author. Email: sheshanath.bhosale@monash.edu

ISSN 1061-0278 print/ISSN 1029-0478 online

DOI: 10.1080/10610278.2011.575467
http://www.informaworld.com

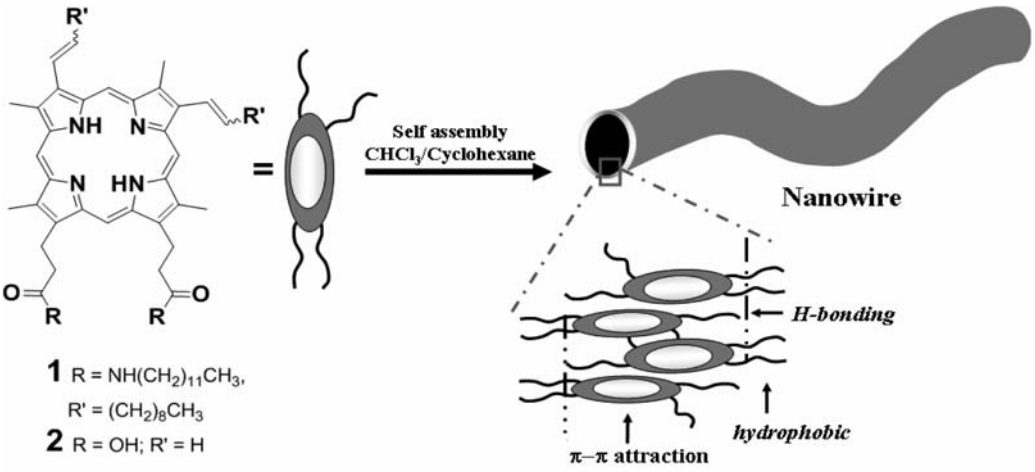


Figure 1. The proposed self-assembled 'nanowires' formed from the tetraalkyl-substituted protoporphyrin **1** in $CHCl_3$/cyclohexane.

1-undecene using the second-generation Grubbs' catalyst in dry tetrahydrofuran (THF) under an argon atmosphere gave the target compound **1** in 78% yield (Scheme 1). While the cross metathesis appears to be efficient, a mixture of *E* and *Z* geometric isomers (80:20) is formed at each alkene as evinced by $^1$H NMR spectroscopy.

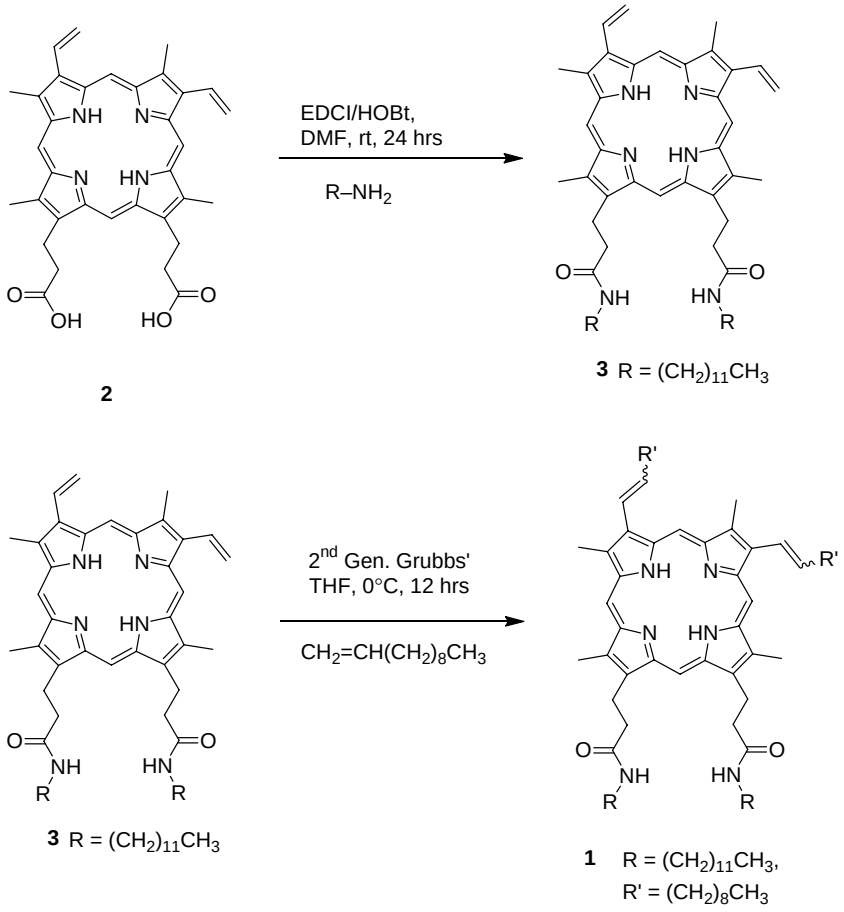


Scheme 1. Synthesis of **1** from protoporphyrin IX.

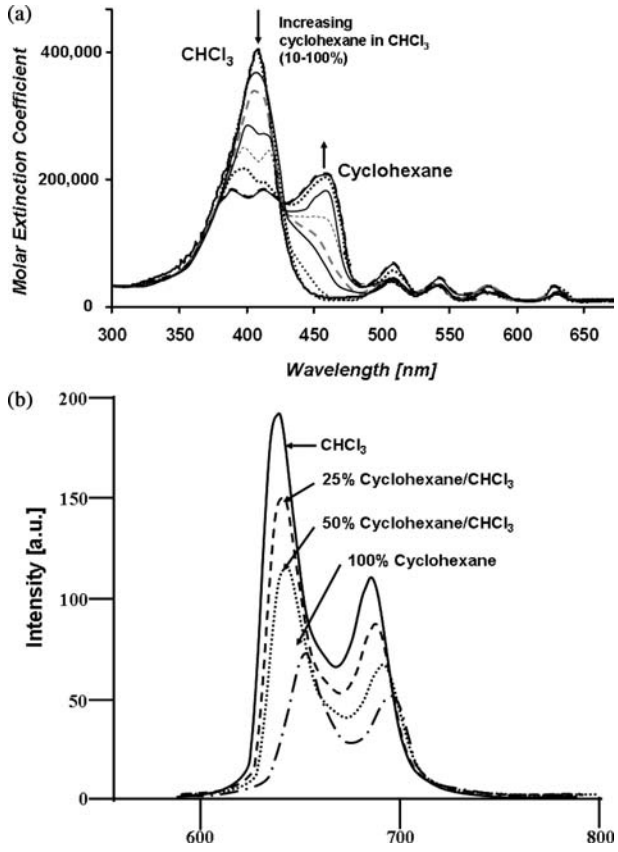


Figure 2. Spectroscopic characterisation of **1** ($4 \times 10^{-5}$ M) in $CHCl_3$ with varying concentration of cyclohexane (0–100%): (a) electronic absorption and (b) emission spectra ($\lambda_{ex} = 420$ nm).

### *UV/vis and fluorescence spectroscopy*

Protoporphyrin **1** was found to be very soluble in chloroform ($CHCl_3$) resulting in a sharp absorption spectra consistent with the presence of monomeric units in this solvent. The absorption spectra are characterised by an intense Soret band at 406 nm ($\varepsilon = 4 \times 10^5\,M^{-1}\,cm^{-1}$), together with four weaker Q bands at 506, 542, 577 and 630 nm (Figure 2(a)). The measurement of differing ratios of cyclohexane to chloroform solutions of **1** by absorption spectroscopy confers significant changes in the absorption band structure (Figure 2(a)). The changes are attributed to aggregation effects in which a reduction in the peak intensity, along with a significant redshift of the absorption maximum and a loss of the fine structure, is seen at higher percentage volume of cyclohexane. When the ratio of cyclohexane is increased to 90% v/v, the Soret band appears at 456 nm along with the usual Q bands (508, 547, 583 and 637 nm). At an equal volume ratio of $CHCl_3$/-cyclohexane, the conversion is halfway. It can be seen that the low-energy Soret band at 456 nm increases gradually, while the Soret band at 406 nm, associated with monomer, decreases gradually with a clean single isosbestic point at or around 423 nm. These phenomena are associated with J-type aggregation (*35*). On the addition of 10% cyclohexane very slow growth takes place. Above 80% v/v cyclohexane in chloroform the spectra remain unchanged, indicating that the aggregation process reaches a steady state. The rapid evolution of the UV–vis spectra demonstrates a fast nucleation process followed by facile growth.

The fluorescence emission spectrum of **1** shows two typical strong bands at 615 and 689 nm on excitation at 420 nm in $CHCl_3$ (Figure 2(b)). The aggregation features of compound **1** in solution have been studied by varying the concentration of cyclohexane in $CHCl_3$ (0, 25, 50 and 100%). Injection of a minimum volume of concentrated chloroform solution of **1** into cyclohexane leads to the formation of two broadened bands at 650 and 705 nm (Figure 2(b)). It can be seen that the fluorescence emission is red-shifted in cyclohexane with respect to that of the species existing in $CHCl_3$ also supporting J-type aggregation of **1**. These features suggest the formation of side-by-side $\pi$ stacks of porphyrin chromophores in a similar effect observed in the case of J aggregation in tetraphenylporphyrin and other similar type of chromophores (*35–37*), and prompted us to further investigate the nature of the aggregates of **1** at or around the point of aggregation using transmission electron microscopy (TEM) and atomic force microscopy (AFM).

### *TEM, AFM and X-ray diffraction measurements*

TEM imaging was performed to better characterise the structure of the aggregates of protoporphyrin **1**. Samples of **1** ([**1**] = 0.5 μM) in $CHCl_3$/cyclohexane (1:9, v/v) were deposited on a carbon grid providing direct visualisation of the self-assembled entities as several micrometre long nanowires (Figure 3). The nanowires thus obtained show quite uniform widths and thickness. The average width is 20 nm and the length is in the range of a few tens of micrometres, leading to an aspect ratio (length over width) in a magnitude of 100 at concentration 0.5 μM (Figure S1, available online). In some instance, the nanowires are observed in a giant agglomerate form indicating the presence of strong cohesion among them. Note that if the self-assembly is undertaken at a higher concentration of **1** (0.7 and 1 μM), TEM images clearly indicate that the nanowire structure consists of bundles that are 40–80 nm in diameter (Figure S2, available online). The observed width of 20 nm is larger than the size of each component molecule, which indicates that **1** is into more than a 1D array.

Samples of **1** prepared for AFM measurements ([**1**] = 0.5 μM) in $CHCl_3$/cyclohexane (1:1 and 1:9, v/v) were spin-coated on a plasma-cleaned silica (111) wafers and examined by tapping mode at ambient conditions. AFM images of **1** from $CHCl_3$/cyclohexane (1:1, v/v) give fibril nanostructure morphologies. The lengths of fibrils exceed several micrometres and the widths are approximately 6–7 nm (Figure 4). X-ray diffraction measurements

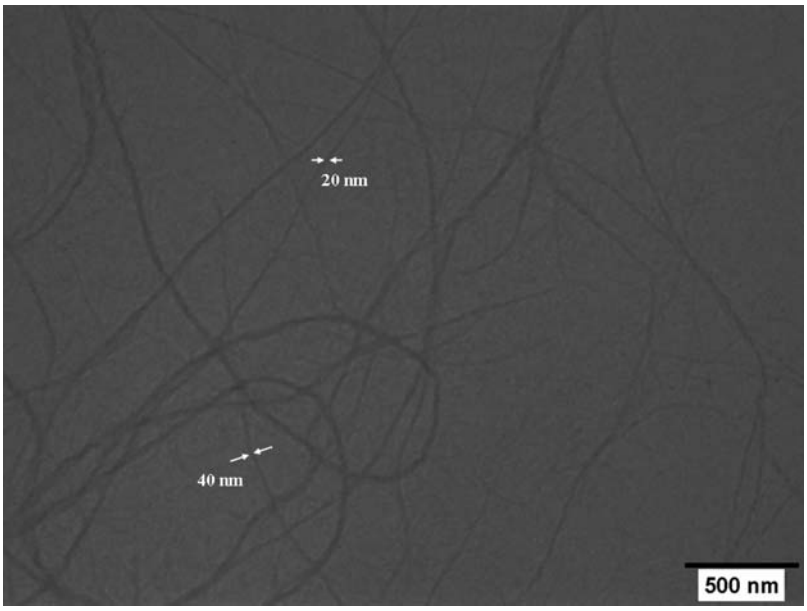


Figure 3. Transmission electron micrograph of a 0.5 μM dispersion of **1** in $CHCl_3$/cyclohexane (1:9, v/v).

were carried out to identify the mesophase of nanostructure **1** in solution.

The X-ray diffraction measurement of the protoporphyrin is provided in Figure 4(d) (*21*). The diffraction broad halo peak around $2\theta = 7.3^\circ$ was seen, indicating that this phase should be mesomorphic. However, the sharp peaks at $3.8^\circ$ are detected in the wide-angle region which can result from the existence of a columnar structure in a smectic layer. Additionally, the ratio of *d* spacing corresponding to the two reflection peaks in the small-angle region is 1:1/4, which illustrates that the mesophase has lamellar type ordering structure (smectic type of ordering) with an

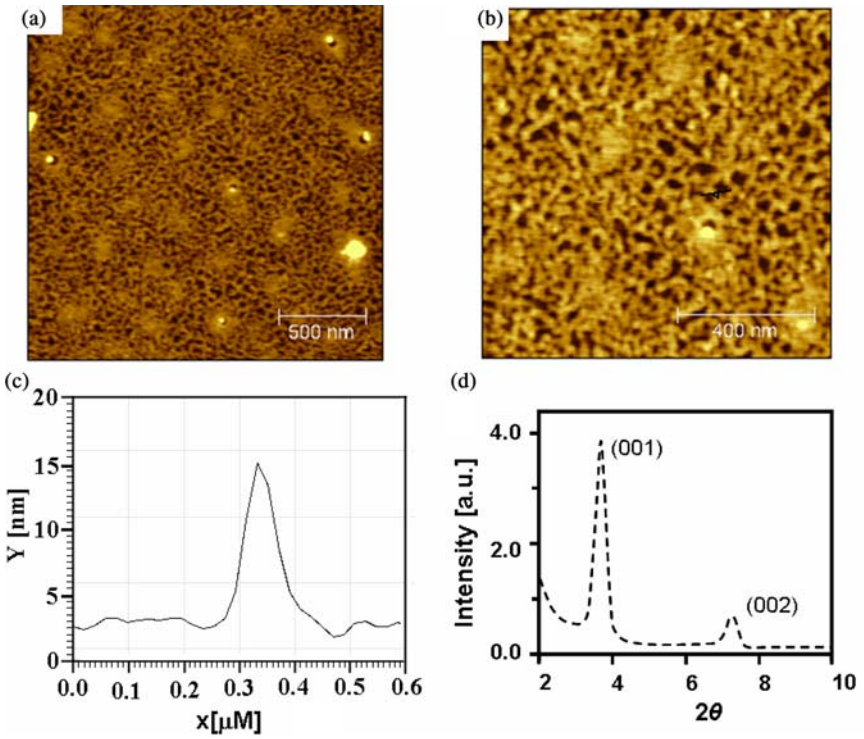


Figure 4. (a) Large-area AFM image of **1** (0.5 μM) self-assembled into micellar fibrils, prepared from $CHCl_3$/cyclohexane solution (1:1, v/v). (b) A higher-magnification image of micellar fibrils. (c) Height profile for (b) clearly shows ratio to height c.a. 6 nm. (d) X-ray diffraction traces of a protoporphyrin derivative **1**.

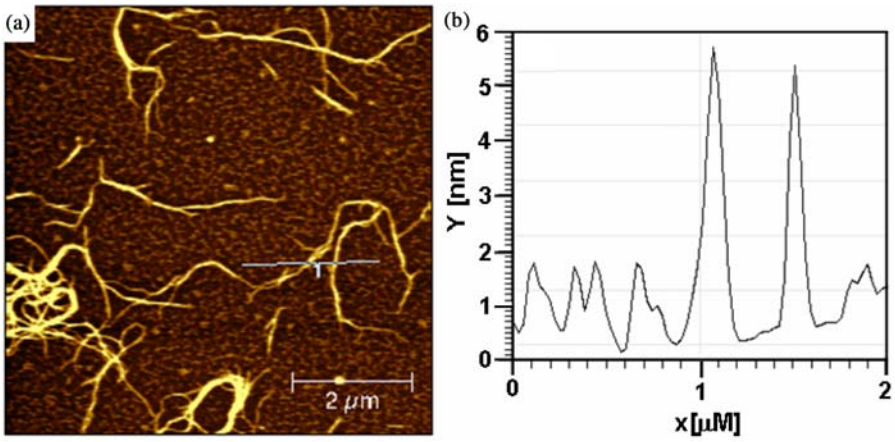


Figure 5. (a) AFM image of self-assembled nanowires of protoporphyrin **1** (0.5 μM) from 1:9, v/v $CHCl_3$/cyclohexane solution and (b) height profile for (a).



interlamellar spacing of 21.5 Å. This distance is about 20% shorter than the total length of a protoporphyrin **1** molecule (along the long axis). While the structure is unknown, the results obtained are consistent with our recently reported self-assembly process for a naphthalene diimide derivative, which form worm-like nanostructure in a mixed organic solvents (*38*).

The AFM images also exhibit a highly developed and intertwined nanowire structure with widths of approximately 20–40 nm (Figure 5(a)). The average height and width of the smallest resolved nanowires are 20 nm, corresponding to the thicker nanowires observed by TEM (Figure 2). The heights of profiles are 6 and 5.5 nm consistent with the thinnest of the nanostructures and typical topography of a nanowire (Figure 5(b)). In some areas, the nanowires show twisted conformations with the edge lifted up perpendicular to the substrate, clearly revealing the grouped nature of the wire morphology of the assembly (Figure S5(b), available online). The ratio of the diameter and height of the nanostructures formed by **1** also suggests a flattening upon being transferred from solution to silicon surface (*32–34*).

Decreasing the amount of cyclohexane to less than 50% v/v does not give any detailed micro-or nanostructure within the time frame of the experiment, indicating the delicate balance of solvophobicity that is important. Interestingly, no specific change was observed for **2** in which neither the northern part nor the southern part is alkylated at any proportions of $CHCl_3$/cyclohexane mixes indicating the subtleties of the '*solvo-controlled*' self-assembly process, as both the aromatic core and lipophilic groups act cooperatively to lead to the final aggregates of **1**. We speculate that the self-assembly is predominantly driven by π–π attractions amongst the porphyrin cores with intermolecular lipophilic interactions leading to further aggregation. We propose the overall structure may also be stabilised by the intermolecular H bonds between the amide groups in **1** (Figure 1).

## Experimental

### *Materials and measurement*

Protoporphyrin IX, dodecyl amine, EDCI, HOBt, 1-udecene, second-generation Grubbs' catalyst, chloroform ($CHCl_3$), DMF, THF, cyclohexane and dichloromethane were purchased from Sigma-Aldrich and used without purification. UV–vis absorption spectra were recorded on a PerkinElmer Lambda 40 p spectrometer. The solvents for spectroscopic studies were of spectroscopic grade and used as received. Self-assembled samples were prepared by dissolving amphiphile **1** in concentrated $CHCl_3$. The sample solution was kept at room temperature for few hours before TEM and AFM measurements. $^1$H and $^{13}$C NMR spectra were recorded with a Varian Gemini (300 MHz for $^1$H NMR and 75 MHz for $^{13}$C NMR), a Varian Mercury (400 MHz for $^1$H NMR and 100 MHz for $^{13}$C NMR) or a Varian Unity Inova (500 MHz for $^1$H NMR and 125 MHz for $^{13}$C NMR) spectrometers. Chemical shifts are reported in parts per million downfield from tetramethylsilane (TMS; $\delta = 0$) at 300 K using $CDCl_3$ as solvent and internal standard unless otherwise indicated. IR spectra were recorded with a PerkinElmer 1600 FT-IR (UATR) spectrometer. Unless stated otherwise, column chromatography was carried out on silica gel 60 (Fluka, 40–63 μM), melting points on a heating table from Reichert (Austria). Analytical TLC was performed in silica gel 60 (Fluka, 0.2 μM). Other reagents were purchased from Aldrich and were used without further purification.

### *Synthesis of protoporphyrin IX amphiphile 1*

#### *Synthesis of compound 3*

Protoporphyrin IX **2** (100 mg, 0.17 mmol) and HOBt (71 mg, 0.53 mmol) were combined in DMF (10 mL) under

argon atmosphere. The solution was cooled to 0°C and stirred for 40 min, then EDCI (100 mg, 0.53 mmol) was added and solution was stirred for 60 min at 0°C. 1-Dodecyl amine (130 mg, 0.53 mmol) was added from DMF (2 mL) at once and the resulting solution was stirred for additional 4 h at 0°C, then warmed to room temperature and left to stir for further 24 h. After this time, the reaction solvent (DMF) was removed by rotary evaporation in reduced pressure, then gummy reaction mixture was taken in dichloromethane (100 mL) and washed with 10% $NaHCO_3$ (2 × 30 mL), 0.1 M HCl (20 mL), followed by water (20 ml) and brine (20 mL); organic solvent was dried over sodium sulphate, filtered and concentrated using a rotary evaporation; purification of crude was carried out on flash silica gel chromatography ($SiO_2$); column elute first with chloroform followed by 4% methanol in chloroform gives dark violet crystalline material of **3** (140 mg, 88%), MP > 350°C. $^1$H NMR ($CDCl_3$, 400 MHz) $\delta$: 10.09–9.90, 4H, m; 4 × methine protons; 8.20, m, 2H 2 × $CHCH_2$; 6.45–6.15, 4H, m, 2 × $CHCH_2$; 5.38, 2H, 2s, CONH; 4.35, 4H, m, 2 × $CH_2CH_2CONH$; 3.78–3.35, 12H, m, 4 × ring methyl; 3.12–2.90, 4H, m, $NHCH_2CH_2$; 2.72–2.53, 4H, m, 2 × $CH_2CH_2CONH$; 2.51–2.42, 4H, m, 2 × $NHCH_2CH_2$; 1.58–0.69, 42H, m, alkyl chain; − 3.89, 2H, br s, 2 × ring NH. $^{13}$C NMR ($CDCl_3$, 100 MHz) $\delta$: 171.5, 145.9, 138.7, 138.5, 136.3, 130.0, 120.1, 118.4, 98.0, 97.7, 97.1, 96.7, 58.0, 40.8, 36.6, 30.0, 29.6, 29.3, 26.8, 14.1, 12.5, 11.5. IR ($CDCl_3$) cm$^{-1}$: 1642 for CONH, 1350, 1600, 1100, 1250, 1060, 960, 990, 835, 844, 772, 805. HRMS: Calcd $C_{58}H_{84}N_6O$ 2896.6656; found 2896.6655.

### *Synthesis of protoporphyrin target derivative (**1**)*

Compound **3** (50 mg, 44 μmol) and 1-undecene (15 mg, 97 μmol) were combined in dry THF (10 mL) under argon atmosphere. Then a solution of second-generation Grubbs' catalyst (6 mg, 0.01 mmol) in THF (2 mL) was added via syringe to the reaction mixture. The reaction mixture was refluxed mildly under argon atmosphere for 12 h. After this time, the reaction solvent (THF) was removed by rotary evaporation in reduced pressure, then solid reaction mixture was taken in dichloromethane (50 mL) and washed with 10% $NaHCO_3$ (2 × 30 mL), 0.1 M HCl (20 mL), followed by water (20 ml) and brine (20 mL); organic solvent was dried over sodium sulphate, filtered and concentrated using a rotary evaporation; purification of crude was carried out on flash silica gel chromatography ($SiO_2$); and column elute first with dichloromethane followed by 2% methanol in dichloromethane gives **1** dark violet crystalline material (51 mg, 78%), MP > 350°C. $^1$H NMR ($CDCl_3$, 400 MHz) $\delta$: $^1$H NMR ($CDCl_3$, 400 MHz) $\delta$: 10.09–9.96, 4H, m; 4 × methine protons; 8.20, m, 2H, 2 × CHCH; 6.45–6.15, 2H, m, 2 × $CHCH_2$; 5.38, 2H, 2s, CONH; 4.35, 4H, m, 2 × $CH_2CH_2CONH$; 3.94–3.75, 12H, m, 4 × ring methyl; 3.45–2.90, 8H, m, $NHCH_2CH_2$ and 2 × $CH_2CH_2CONH$; 2.35–2.14, 4H, m, 2 × $CH_2CH_2CONH$; 1.89–1.77, 4H, m, 2 × $NHCH_2CH_2$; 1.75–0.72, 76H, m, alkyl chain; − 3.96, 2H, s, 2 × ring NH. $^{13}$C NMR ($CDCl_3$, 125 MHz) $\delta$: 173.1, 145.9, 138.7, 138.5, 136.3, 130.0, 129.4, 121.3, 120.1, 118.4, 98.0, 97.7, 97.1, 96.7, 58.0, 40.8, 36.6, 30.0, 29.7, 29.6, 29.3, 26.8, 26.7, 22.7, 21.2, 14.1, 12.5, 11.5. IR ($CDCl_3$) cm$^{-1}$: 1645 for CONH, 1350, 1600, 1100, 1250, 1060, 960, 990, 835, 844, 772, 805. HRMS: Calcd $C_{76}H_{120}N_6O_2$ 1148.9473; found 1148.9474.

### *Self-assembled standard protoporphyrin **1** solution*

A 0.1 mL sample of a stock solution of **1** (0.7 μM, $CHCl_3$) was diluted in $CHCl_3$ (0.9 mL). To the homogeneous solution, 9 mL of spectroscopic grade cyclohexane was added very fast under continuous magnetic stirring at 25°C. The solution became opaque immediately. The dispersion was then kept under continuous magnetic stirring for 1 h using magnetic needle. Finally, the dispersion was kept in dark and used for measurements of AFM and TEM. In another experiment, **1** in $CHCl_3$/cyclohexane (1:1, v/v): 1.0 mL of spectroscopic grade of cyclohexane was added to 1.0 mL solution of **1** (2 μM) in $CHCl_3$ at 25°C following the similar process as above.

### *UV–vis and fluorescence spectroscopy*

Stock solutions ($3.99 \times 10^{-5}$ M) of **1** were made in $CHCl_3$. The solutions were allowed to equilibrate for 2 h prior to the spectroscopic measurements.

### *Transmission electron microscopy (TEM)*

A droplet (5 μL) of the freshly prepared solution [above self-assembled standard protoporphyrin **1** in $CHCl_3$/cyclohexane (1:9, v/v)] was placed on hydrophilised carbon films on copper wire grids (60 s plasma treatment at 8 W using a BALTEC MED 020 device). Excess fluid was blotted off and air-dried on the grids. Microscopy was carried out using a Philips CM12 TEM operated at 100 kV accelerating voltage at a low electron dose (< 100 e/Å).

### *Atomic force microscopy (AFM)*

Samples were characterised using an AFM from Agilent Technologies (5500 AFM). Micromach ultra-sharp probes with silica wafer coating for enhanced reflectivity (NSC15/AIBS), with a typical resonance frequency of 325 kHz and a force constant of 40 N/m, were used for imaging. All samples were measured at room temperature in air environments. Sample of protoporphyrin **1** were spin-coated onto silica wafer at 2000 rpm from the mixture of $CHCl_3$/cyclohexane (1:1 or 1:9, v/v). The of nanowires diameter and height were performed by measuring the mean horizontal distance and height of wires (see Figures 4 and S4–S5, available online). Figure S4 of the

Supplementary Information, available online, shows AFM images of the self-assembled supramolecular micellar fibrils of **1** from $CHCl_3$/cyclohexane (1:1, v/v).

### *X-ray diffraction spectroscopy*

X-ray diffraction was performed on a Siemens D500 diffractometer X-ray Diffraction Spectrometer, in which a copper–$K_\alpha$ radiation (Cu $K\alpha_{avg}$, $\lambda = 1.5418$ Å) was used. The samples for X-ray measurement were prepared on glass cover slips by drop casting, followed by drying at room temperature.

## Conclusion

We have demonstrated the aggregation of alkyl-substituted protoporphyrin derivative, self-assembled in J-type aggregates into narrowly dispersed nanowires and macroscopic nanowire bundles in varying concentration of $CHCl_3$/cyclohexane. Although the exact step-by-step growth of the molecular wires formation is not yet known, it is evident that the presence of hydrophobic tail on both ends plays important role in the self-assembled process. We are also currently producing the protoporphyrin nanowires from zinc and tin(IV) complexes to measure electric conductivities of cation and anion π-radical stacks (*39*).

## Acknowledgements

Sid.V.B. would like to thank CSIR, New Delhi, India, for financial assistance [Project no. 01 (2283)/08/EMR-II] and Shesh.V.B. and S.J.L. gratefully acknowledge the Australian Research Council for support under the Discovery Programme (DP0878756 and DP0878220). We also thank B. Patro and P. Varghese (IIT Bombay) for TEM measurements.

## References

(1) Lehn, J.-M. *Science* **2002**, *295*, 2400–2403.
(2) Aratani, N.; Kim, D.; Osuka, A. *Acc. Chem. Res.* **2009**, *42*, 1922–1934.
(3) Drain, C.M.; Goldberg, I.; Sylvain, I.; Falber, A. *Top. Curr. Chem.* **2005**, *245*, 55–88.
(4) Balaban, T.S. *Acc. Chem. Res.* **2005**, *38*, 612–623.
(5) Holten, D.; Bocian, D.F.; Lindsey, J.S. *Acc. Chem. Res.* **2002**, *35*, 57–69.
(6) Tsuda, A.; Osuka, A. *Science* **2001**, *293*, 79–82.
(7) Gust, D.; Moore, T.A.; Moore, A.L. *Acc. Chem. Res.* **2001**, *34*, 40–48.
(8) Leslie-Anne, F.; Meike, S.; Nikolai, W.; Mihaela, E.; Thomas, J.A.; Francois, D. *Chem. Eur. J.* **2009**, *15*, 11139–11150.
(9) Bhosale, S.V.; Kalyankar, M.B.; Langford, S.J.; Bhosale, S.V.; Oliver, R.F. *Eur. J. Org. Chem.* **2009**, 4128–4134.
(10) Grill, L.; Dyer, M.; Lafferentz, L.; Persson, M.; Peters, M.V.; Hecht, S. *Nat. Nanotechnol.* **2007**, *2*, 687–691.
(11) Wang, Z.; Ho, K.J.; Medforth, C.J.; Shelnutt, J.A. *Adv. Mater.* **2006**, *18*, 2557–2560.
(12) Li, W.-L.; Jiang, D.-L.; Suna, Y.; Aida, T. *J. Am. Chem. Soc.* **2005**, *127*, 7700–7702.
(13) Wang, Z.; Medforth, C.J.; Shelnutt, J.A. *J. Am. Chem. Soc.* **2004**, *126*, 15954–15955.
(14) Tiede, D.M.; Zhang, R.; Chen, L.X.; Yu, L.; Lindsey, J.S. *J. Am. Chem. Soc.* **2004**, *126*, 14054–14062.
(15) Balaban, T.S.; Eichhofer, A.; Lehn, J.M. *Eur. J. Org. Chem.* **2000**, 4047–4057.
(16) Maier, S.; Fendt, L.-A.; Zimmerli, L.; Glatzel, T.; Pfeiffer, O.; Diederich, F.; Meyer, E. *Small* **2008**, *4*, 1115–1118.
(17) Chen, X.; Kang, S.; Kim, M.J.; Kim, J.; Kim, Y.S.; Kim, H.; Chi, B.; Kim, S.-J.; Lee, J.Y.; Yoon, J. *Angew. Chem. Int. Ed.* **2010**, *49*, 1422–1425.
(18) Tanaka, H.; Ikeda, T.; Yamashita, K.; Takeuchi, M.; Shinkai, S.; Kawai, T. *Langmuir* **2010**, *26*, 210–214.
(19) Haino, T.; Fujii, T.; Watanabe, A.; Takayanagi, U. *Proc. Natl. Acad. Sci. USA* **2009**, *106*, 10477–10481.
(20) Corbett, P.T.; Leclaire, J.; Vial, L.; West, K.R.; Wietor, J.-L.; Sanders, J.K.M.; Otto, S. *Chem. Rev.* **2006**, *106*, 3652–3711.
(21) Camara-Campos, A.; Hunter, C.A.; Tomas, S. *Proc. Natl. Acad. Sci. USA* **2006**, *103*, 3034–3038.
(22) Guldi, D.M.; Zerbetto, F.; Georgakilas, V.; Prato, M. *Acc. Chem. Res.* **2005**, *38*, 38–43.
(23) Tomizaki, K.-Y.; Yu, L.; Wei, L.; Bocian, D.F.; Lindsey, J.S. *J. Org. Chem.* **2003**, *68*, 8199–8207.
(24) Tsuda, A.; Sakamoto, S.; Yamaguchi, K.; Aida, T. *J. Am. Chem. Soc.* **2003**, *125*, 15722–15723.
(25) Bhosale, S.V.; Bhosale, S.V.; Kalyankar, M.B.; Langford, S.J.; Lalander, C.H. *Aus. J. Chem.* **2010**, *63*, 1326–1329.
(26) Koti, A.S.R.; Periasamy, N. *Chem. Mater.* **2003**, *15*, 369–671.
(27) Okada, S.; Segawa, H. *J. Am. Chem. Soc.* **2003**, *125*, 2792–2796.
(28) Scolaro, L.M.; Castriciano, M.; Romeo, A.; Patané, S.; Cefalí, E.; Allegrini, M. *J. Phys. Chem. B* **2002**, *106*, 2453–2459.
(29) Fuhrhop, J.-H.; Koning, J. *Membranes and Molecular Assemblies: The Synkinetic Approach*; Stoddart, J.F., Ed.; The Royal Society of Chemistry: Cambridge, UK, 1994.
(30) Fuhrhop, J.-H.; Bindig, U.; Siggel, U. *J. Am. Chem. Soc.* **1993**, *115*, 11036–11037.
(31) Fuhrhop, J.-H.; Bindig, U.; Rosengarten, B.; Siggel, U. *Polym. Adv. Technol.* **1995**, *6*, 168–177.
(32) Castella, M.; Lopez-Calahorra, F.; Velasco, D.; Finkelmann, H. *Chem. Commun.* **2002**, 2348–2349.
(33) Schenning, A.P.H.J.; Benneker, F.B.G.; Geurts, H.P.M.; Liu, X.Y.; Nolte, R.J.M. *J. Am. Chem. Soc.* **1996**, *118*, 8549–8552.
(34) Bindig, U.; Schulz, A.; Fuhrhop, J.-H.; Siggel, U. *New J. Chem.* **1995**, *19*, 427–435.
(35) Okada, S.; Segawa, H. *J. Am. Chem. Soc.* **2003**, *125*, 2792–2796.
(36) Takeuchi, M.; Tanaka, S.; Shinkai, S. *Chem. Commun.* **2005**, 5539–5541.
(37) Kitahama, Y.; Kimura, Y.; Takazawa, K. *Langmuir* **2006**, *22*, 7600–7604.
(38) Bhosale, S.V.; Jani, C.H.; Lalander, C.H.; Langford, S.J. *Chem. Commun.* **2010**, *46*, 973–975.
(39) Fuhrhop, J.-H.; Kadish, D.G.; Davis, D.G. *J. Am. Chem. Soc.* **1973**, *95*, 5140–5147.